



# Synthesis, magnetic properties and Mössbauer spectroscopy for the pyrochlore family $\text{Bi}_2\text{BB}'\text{O}_7$ with $\text{B}=\text{Cr}$ and $\text{Fe}$ and $\text{B}'=\text{Nb}$ , $\text{Ta}$ and $\text{Sb}$

Maria C. Blanco<sup>a</sup>, Diego G. Franco<sup>a,b</sup>, Yamile Jalit<sup>a</sup>, Elisa V. Pannunzio Miner<sup>a</sup>, Graciele Berndt<sup>c</sup>, Andrea Paesano Jr.<sup>c</sup>, Gladys Nieva<sup>b</sup>, Raúl E. Carbonio<sup>a,\*</sup>

<sup>a</sup> INFIQC (CONICET), Dpto. de Fisicoquímica, Fac. de Ciencias Químicas, U.N.C., Córdoba (X5000HUA), Argentina

<sup>b</sup> Centro Atómico Bariloche – CNEA, Av. E. Bustillo 9500, S.C. de Bariloche (8500), R.N., Argentina

<sup>c</sup> Departamento de Física, Universidade Estadual de Maringá, Parana, Brazil

## ARTICLE INFO

Available online 17 December 2011

### Keywords:

Pyrochlores  
Crystal structure  
Magnetism  
Mössbauer spectroscopy  
Displacive disorder

## ABSTRACT

The samples  $\text{Bi}_2\text{BB}'\text{O}_7$ , with  $\text{B}=\text{Cr}$  and  $\text{Fe}$  and  $\text{B}'=\text{Nb}$ ,  $\text{Ta}$  and  $\text{Sb}$  were prepared by solid state method. The crystallographic structure was investigated on the basis of X-ray powder diffraction data. Rietveld refinements show that the crystal structure is cubic, space group  $\text{Fd-}3\text{m}$ . The  $\text{Bi}^{3+}$  cation on the eight-coordinate pyrochlore A-site shows displacive disorder, as a consequence of its lone pair electron configuration. There is also a considerable A-site disorder shown by Rietveld Analysis and confirmed in the case of the iron containing samples with Mössbauer spectroscopy. The magnetic measurements show paramagnetic behavior at all temperatures for the Cr oxides. The Fe pyrochlores show antiferromagnetic order around 10 K.

© 2011 Elsevier B.V. All rights reserved.

## 1. Introduction

Pyrochlore oxides are being the subject of renewed interest because of their many interesting applications. Specifically those with formula  $\text{A}_2\text{BB}'\text{O}_7$  were recently informed to be alternative cathodes for IT-SOFCs [1]. Proton conductivity has also been observed in doped  $\text{Sm}_2\text{Sn}_2\text{O}_7$  [2] and dielectric properties were informed for doped  $\text{Bi}_{1.5}\text{Zn}_{0.92}\text{Nb}_{1.5}\text{O}_{6.92}$  [3]. Many other important applications make the synthesis of new pyrochlore oxides and their fundamental studies a very interesting area of research. The typical pyrochlore compound has the general formula  $\text{A}_2\text{B}_2\text{O}_7$ , with a cubic crystal structure  $\text{Fd-}3\text{m}$  (SG # 227), and it is well described as  $\text{A}_2\text{B}_2\text{O}_6\text{O}'$  comprising two interpenetrating sublattices with the formulae  $\text{A}_2\text{O}'$  and  $\text{B}_2\text{O}_6$ . Non spherical lone pair active cations (like  $\text{Bi}^{3+}$ ) inside the classic cubic pyrochlore structure, instead of the classic off-centered coordination polyhedra that generates polar structures, it can be accommodated through incoherent displacive disorder [4]. Their appearance is rationalized by a static displacement of the A ions toward the surrounding ring of O atoms [5]. It has been demonstrated that for certain pyrochlore compositions, the phase becomes stable only when a substitutional disorder is present in the A-cation site [4], with small B ions surprisingly occupying the large A-site. This site disorder is well-known for lone pair active cations such as  $\text{Tl}^{+1}$ ,

\* Corresponding author. Tel.: +54 351 433 4169/80; fax: +54 351 433 4188.  
E-mail address: carbonio@mail.fcq.unc.edu.ar (R.E. Carbonio).

$\text{Sn}^{2+}$ , and  $\text{Bi}^{3+}$  [6–9]. In the present article, the synthesis of new  $\text{Bi}_2\text{BB}'\text{O}_7$  pyrochlores with a combination of both, a magnetic ion and a spectator ion on the B-sites (where  $\text{B}=\text{Cr}$  and  $\text{Fe}$  and  $\text{B}'=\text{Nb}$ ,  $\text{Ta}$  and  $\text{Sb}$ ) have been selected as an interesting family to study their fundamental physical properties, displacive and substitutional A-cation site disorder. This stoichiometry allows combine a magnetic  $\text{B}^{3+}$  cation with a diamagnetic  $\text{B}'^{5+}$  one. The use of iron allows us to use Mössbauer spectroscopy to corroborate the crystallographic conclusions. Magnetic properties are also discussed.

## 2. Experimental

The  $\text{Bi}_2\text{BB}'\text{O}_7$  compounds were synthesized by solid state reaction from stoichiometric quantities of the binary oxides  $\text{Bi}_2\text{O}_3$ ,  $\text{Cr}_2\text{O}_3$ ,  $\text{Fe}_2\text{O}_3$ ,  $\text{Nb}_2\text{O}_5$ ,  $\text{Ta}_2\text{O}_5$  and  $\text{Sb}_2\text{O}_3$ . The samples were mixed in an agate mortar and calcined in air atmosphere. One thermal treatment for 12 h at 975 °C has been used for Sb pyrochlores, while Nb and Ta ones required three consecutive thermal treatments for 24 h at 1000 °C. X-ray powder diffraction data (XRPD) was measured on a PANalytical's X'Pert PRO diffractometer (40 keV, 40 mA), in Bragg–Brentano reflection geometry with  $\text{CuK}_\alpha$  radiation ( $\lambda=1.5418 \text{ \AA}$ ) at room temperature. Mössbauer spectra were taken at room temperature, from a constant acceleration spectrometer with a  $^{57}\text{Co}(\text{Rh})$  source, using absorbers with nearly  $67 \text{ mg/cm}^2$ . Magnetization ( $\chi$ ) was measured as a function of Temperature ( $T$ ) in a superconducting

quantum interference device magnetometer (SQUID), between 5 and 300 K, after cooling in the absence of an applied field (zero-field cooled, ZFC) and after cooling in a magnetic field (field-cooled, FC).

### 3. Results and discussion

#### 3.1. Crystal structure

All materials were obtained as polycrystalline powders. Sample purity was around 98–99% in all cases. Initially the structures were refined assuming the ideal pyrochlore structure type. Although the structural refinement was satisfactory (see Fig. 1 and Table 1) the refined isotropic temperature factor for Bi ions was unusually large.

Furthermore, some observed experimental peaks at high angles were reproduced with zero intensity, although the Bragg positions were allowed. These facts are in agreement with the possibility of static displacive disorder for  $\text{Bi}^{3+}$  ion [4,5]. We consider a model with displacement of both,  $\text{Bi}^{3+}$  and  $\text{O}(2)$  ( $\text{O}'$ ) which lead to a better fit of the experimental data and drop the isotropic temperature factors. In Table 1 we compare this model with the ideal cubic model. In Fig. 1 we show the Rietveld refinement of XRPD data for  $\text{Bi}_2\text{CrNbO}_7$  including static displacive

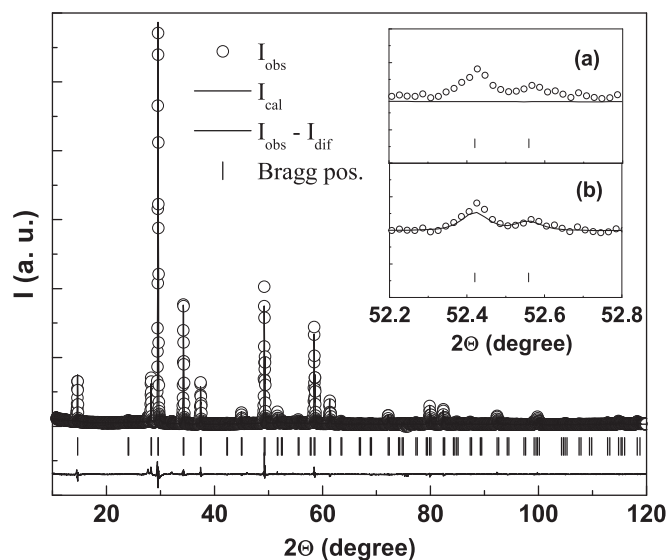


**Fig. 1.** Rietveld refinement of XRPD pattern for  $\text{Bi}_2\text{CrNbO}_7$ , with Bi and  $\text{O}(2)$  displaced. Inset: detail of the 442 reflection for the cubic ideal model (a) and for the displacive one (b), showing the improvement of the fit taking into account the displacive disorder.

**Table 1**

Rietveld refinements results of  $\text{Bi}_2\text{CrNbO}_7$  for the ideal cubic model with Bi fixed at  $(1/2, 1/2, 1/2)$ , and the disordered model with Bi displaced at  $(0, y, -y)$  and  $\text{O}(2)$  displaced at  $(x, x, x)$ .

| atom  | Site | x          | y         | Z         | Biso    |
|---|------|------------|-----------|-----------|---------|
| Bi/Cr   | 16d  | 0.5        | 0.5       | 0.5       | 2.21(1) |
| Nb/Cr   | 16c  | 0          | 0         | 0         | 1.66(1) |
| O(1)  | 48f  | 0.2967(7)  | 0.125     | 0.125     | 1.73(1) |
| O(2)  | 8b   | 0.375      | 0.375     | 0.375     | 1.06(1) |
| <b>Ideal model: <math>a=10.4638(2)</math>, <math>R_p=9.38</math>, <math>R_{wp}=13.7</math></b>      |      |            |           |           |         |
| Bi/Cr   | 96h  | 0          | 0.2229(2) | 0.7770(2) | 0.33(1) |
| Nb/Cr   | 16c  | 0          | 0         | 0         | 0.97(2) |
| O(1)  | 48f  | 0.31345(7) | 0.125     | 0.125     | 2.54(1) |
| <b>Disordered model: <math>a=10.4634(2)</math>, <math>R_p=7.23</math>, <math>R_{wp}=10.6</math></b> |      |            |           |           |         |

disorder. Similar results were obtained for the rest of the compounds (not shown).

Finally, A-site cation site disorder [4] was allowed and refined. We show the results of the occupancies for all the compounds in Table 2. The stoichiometry for all materials can be written then as  $\text{VIII}(\text{Bi}_{2-x}\text{B}_x)^{\text{VI}}(\text{B}_{1-y}\text{B}'_{1+y})\text{O}_7$  with  $x$  between 0.06 and 0.29 (roman numbers indicate coordination numbers). Larger A-site disorder was obtained for  $\text{Bi}_2\text{FeNbO}_7$ , this will be later compared with the Mössbauer results.

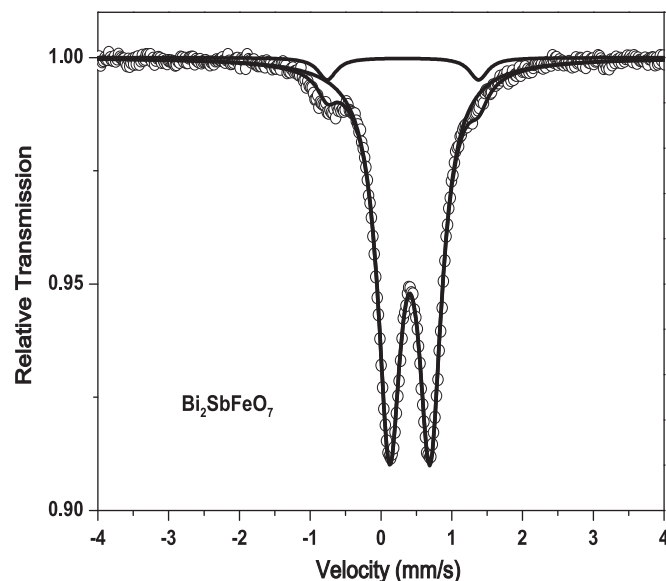
#### 3.2. Mössbauer spectroscopy

Fig. 2 shows the Mössbauer spectrum for the  $\text{Bi}_2\text{FeSbO}_7$  pyrochlore (the rest of the samples show similar spectra). The spectra were fitted using two quadrupolar doublets since higher velocity measurements (not shown) revealed no magnetic components. Table 3 displays the fitted hyperfine parameters for all  $\text{Bi}_2\text{FeB}'\text{O}_7$  samples. The present results are similar to those earlier obtained for the  $\text{Y}_2\text{FeSbO}_7$  pyrochlore [10] and  $\text{Bi}_{2-x}\text{Y}_x\text{FeSbO}_7$  [11]. It is clear that iron ions are located simultaneously in two different sites, the A and B-sites of the pyrochlore structure, thus corroborating the A-cation site disorder obtained by XRPD. Also the Mössbauer absorption area ratios, Doublet A/Doublet B (where A and B refer to the pyrochlore sites), are in good agreement with the result of the X-ray diffraction refinements, larger A-site disorder is also obtained for  $\text{Bi}_2\text{FeNbO}_7$ , and it is larger than the informed for  $\text{Bi}_{1.89}\text{Fe}_{1.16}\text{Nb}_{0.95}\text{O}_{6.95}$  [12]. According to the IS, both sites are occupied by trivalent iron although one of them (Doublet A) has, for every sample, a quadrupole splitting unusually large for  $\text{Fe}^{3+}$ . This could be attributed to the lower

**Table 2**

Occupancies of A and B-sites obtained by Rietveld refinements of XRPD data.

| B' | Site |                                | $\text{Bi}_2\text{CrB}'\text{O}_7$ | $\text{Bi}_2\text{FeB}'\text{O}_7$ |
|----|------|--------------------------------|------------------------------------|------------------------------------|
| Nb | A    | $\text{Bi}^{3+}/\text{B}^{3+}$ | 0.73/0.27                          | 0.71/0.29                          |
|    | B    | $\text{Nb}^{5+}/\text{B}^{3+}$ | 0.33/0.67                          | 0.31/0.69                          |
| Ta | A    | $\text{Bi}^{3+}/\text{B}^{3+}$ | 0.94/0.06                          | 0.86/0.14                          |
|    | B    | $\text{Ta}^{5+}/\text{B}^{3+}$ | 0.63/0.37                          | 0.42/0.58                          |
| Sb | A    | $\text{Bi}^{3+}/\text{B}^{3+}$ | 0.71/0.29                          | 0.82/0.18                          |
|    | B    | $\text{Sb}^{5+}/\text{B}^{3+}$ | 0.39/0.61                          | 0.43/0.57                          |



**Fig. 2.** Mössbauer spectrum for the  $\text{Bi}_2\text{FeSbO}_7$  pyrochlore.

**Table 3**

Hyperfine parameters for  $\text{Bi}_2\text{FeB}'\text{O}_7$ ;  $\Gamma$ : half-width of the absorption line; IS: isomer shift, relative to metallic iron at room temperature; QS: quadrupole splitting; %: subspectral relative area. A and B refer to the pyrochlore sites.

| B/pyrochlore site | IS (mm/s) | QS (mm/s) | $\Gamma$ (mm/s) | %    |
|-------------------|-----------|-----------|-----------------|------|
| Nb/B              | 0.49      | 0.59      | 0.32            | 92.1 |
| Nb/A              | 0.38      | 1.88      | 0.36            | 7.9  |
| Ta/B              | 0.40      | 0.60      | 0.34            | 96.0 |
| Ta/A              | 0.31      | 1.91      | 0.31            | 4.0  |
| Sb/B              | 0.40      | 0.57      | 0.39            | 95.4 |
| Sb/A              | 0.31      | 2.13      | 0.32            | 4.6  |

**Table 4**

$\theta$ ,  $T_N$  and  $\mu_{\text{eff}}$  per  $\text{B}^{3+}$  mol for  $\text{Bi}_2\text{BB}'\text{O}_7$ .

| B                              | $\text{Bi}_2\text{BNbO}_7$ |      | $\text{Bi}_2\text{BTaO}_7$ |      | $\text{Bi}_2\text{BSbO}_7$ |      |
|--------------------------------|----------------------------|------|----------------------------|------|----------------------------|------|
|                                | Cr                         | Fe   | Cr                         | Fe   | Cr                         | Fe   |
| $\mu_{\text{eff}}/\mu\text{B}$ | 3.58                       | 3.28 | 3.95                       | 3.27 | 3.32                       | 4.76 |
| $\theta/\text{K}$              | 1                          | −104 | −6                         | −86  | 7                          | −270 |
| $T_N/\text{K}$                 | —                          | 8.5  | —                          | 8.3  | —                          | 10   |

the derivative of  $\chi$  vs.  $T$ , are 8.3 K for Nb, 8.5 K for Ta, and 10 K for Sb. It is interesting to observe the high calculated frustration factor values,  $f = |\theta|/T_N$ , for the three samples which are 12, 10 and 27 for Nb, Ta and Sb respectively. This high frustration has been observed for other pyrochlores [14]. The larger substitutional disorder present in  $\text{Bi}_2\text{FeNbO}_7$  is responsible of the minor frustration factor compared to  $\text{Bi}_{1.89}\text{Fe}_{1.16}\text{Nb}_{0.95}\text{O}_{6.95}$  [12].

#### 4. Conclusions

The samples  $\text{Bi}_2\text{BB}'\text{O}_7$  (B=Cr and Fe, and B'=Nb, Ta and Sb) were successfully prepared by solid state method. For all materials the crystal structure is cubic, space group Fd-3m. Rietveld adjustments for XRPD showed in all these oxides that Bi and O' have displacive disorder. Also there is a considerable A-site disorder, confirmed by Mössbauer spectroscopy. The magnetic measurements show that Cr oxides are paramagnetic at all temperatures, while Fe pyrochlores show antiferromagnetic order around 10 K.

#### Acknowledgements

R.E.C. thanks ANPCyT, CONICET and SECYT-UNC for financial support. D.G.F. and E.V.P.M. thank CONICET for fellowships. The authors thank CONICET and CNPq for a CIAM collaboration project. We thank J. M. De Paoli for helpful discussions.

#### References

- [1] R. Martínez-Coronado, A. Aguadero, C. de la Calle, M.T. Fernández, J.A. Alonso, J. Power Sources 196 (2011) 4181–4186.
- [2] K.E.J. Eurenium, E. Ahlberg, C.S. Knee, Solid State Ionics 181 (2010) 1577–1585.
- [3] A. Mergen, H. Zorlu, M. Özdemir, M. Yumak, Ceram. Int. 37 (2011) 37–42.
- [4] T.A. Vanderah, I. Levin, M.W. Lufaso, Eur. J. Inorg. Chem. 14 (2005) 2895.
- [5] S. Uma, S. Kodialam, A. Yokochi, N. Khosrovani, M.A. Subramanian, A.W. Sleight, J. Solid State Chem. 155 (2000) 225.
- [6] M. Ganne, M. Tournoux, Mater. Res. Bull. 10 (1975) 1313.
- [7] T. Birchall, A.W. Sleight, J. Solid State Chem. 13 (1975) 118.
- [8] I. Levin, T.G. Amos, J.C. Nino, T.A. Vanderah, C.A. Randall, M.T. Lanagan, J. Solid State Chem. 168 (2002) 69.
- [9] I. Radosavljevic, J.S.O. Evans, A.W. Sleight, J. Solid State Chem. 136 (1998) 63.
- [10] C.K. Matsuda, R. Barco, P. Sharma, V. Biondo, A. Paesano Jr., J.B.M. da Cunha, B. Hallouche, Hyperfine Interact. 175 (2007) 55.
- [11] M.D. Sundararajan, A. Narayanasamy, T. Nagarajan, Solid State Commun. 48 (8) (1983) 657–661.
- [12] W. Miiller, L. Causeret, C.D. Ling, J. Phys. Condens. Matter 22 (2010) 486004.
- [13] M.W. Lufaso, et al., J. Solid State Chem. 179 (2006) 3900.
- [14] J.E. Greedan, J. Mater. Chem. 11 (2001) 37.

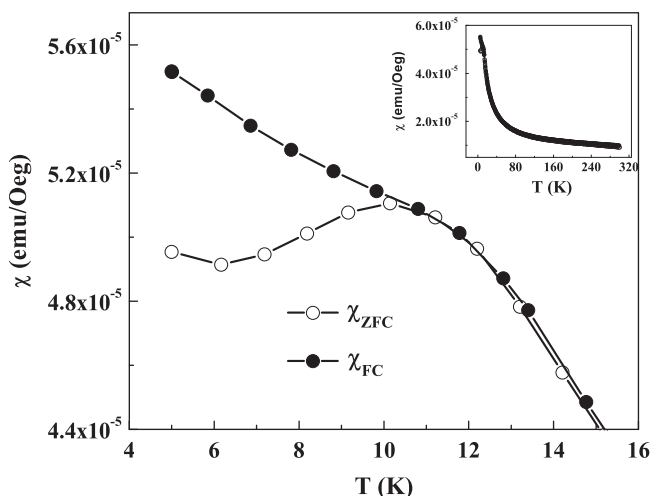


**Fig. 3.**  $\chi$  vs  $T$  for  $\text{Bi}_2\text{FeSbO}_7$  in the low temperature range. The inset shows the complete curve.

symmetry of the A-site. Combination of displacements of A and O' ions produces a largely distorted A-site [13].

#### 3.3. Magnetic measurements

$\text{Bi}_2\text{CrB}'\text{O}_7$  show paramagnetic behavior at all temperatures (not shown). The  $\text{Bi}_2\text{FeB}'\text{O}_7$  pyrochlores also show a paramagnetic behavior, but at low temperatures there is a magnetic order and irreversibility between  $\chi_{\text{ZFC}}$  and  $\chi_{\text{FC}}$ . In Fig. 3 we show the behavior for  $\text{Bi}_2\text{FeSbO}_7$ . The 150 K–300 K range for all samples fit very well with Curie–Weiss law. Table 4 shows experimental Weiss Temperatures ( $\theta$ ), Néel Temperatures ( $T_N$ ) and effective magnetic moments ( $\mu_{\text{eff}}$ ) obtained for all compounds. In the case of  $\text{Cr}^{3+}$  there is a very good agreement between the experimental and calculated spin-only magnetic moment value ( $\mu_{\text{theo}} = 3.87 \mu\text{B}$ ). In contrast, in the iron samples, the experimental spin-only magnetic moments are lower than the calculated for  $\text{Fe}^{3+}$  ( $\mu_{\text{theo}} = 5.92 \mu\text{B}$ ). This has been observed for other pyrochlores [13] and has been attributed to the triangular symmetry of the metal lattices which results in magnetic frustration. The order temperature for  $\text{Bi}_2\text{FeB}'\text{O}_7$  (B'=Nb, Ta and Sb), obtained as the minimum of